Int. J.Nano Dimens. 4(2): 91-104, Autumn 2013
ISSN: 2008-8868

Contents list available at **IJND**

International Journal of Nano Dimension

Journal homepage: *www.IJND.ir*

Nanodimensional AlMCM-41 material for adsorption of dyes: Thermodynamic and kinetic studies

Sh. Sohrabnezhad[1,*]
A. Habibi-Yangjeh[2]
S. Eftekhari[2]

[1]Department of Chemistry, Faculty of Science, University of Guilan, P.O. Box 1914, Rasht, Iran.
[2]Department of Chemistry, University of Mohaghegh Ardabili, P.O. Box 179, Ardabil, Iran.

Received: 21 September 2012
Accepted: 25 November 2012

ABSTRACT

AlMCM-41 was applied for adsorption of methylene blue (MB) and auramine (AU) in single and binary component systems. In the single component systems, AlMCM-41 represents higher adsorption capacity for MB than AU with the maximal adsorption capacity of 2.07×10^{-4} and 1.15×10^{-4} mol/g at 25 ˚C for MB and AU, respectively. In the binary component system, MB and AU exhibit competitive adsorption onto the adsorbent. In single and binary component systems, kinetic and adsorption isotherm studies demonstrate that the data are following pseudo-second-order kinetic model and Langmuir isotherm. Also, in both cases, kinetic data is fairly described by two-step diffusion model. Effect of solution pH on the adsorption of MB and AU in single and binary component systems was studied and the results were described by electrostatic interactions.

Keywords: *Competitive adsorption; Nanodimensional AlMCM-41; Adsorption kinetic; Adsorption isotherm; Methylene blue; Auramine*.

INTRODUCTION

The discharge of dye effluents to the environment, especially to water system, is becoming a major concern due to their toxicity. The origins of these dyes are usually from industries such as textiles, dyestuff manufacturing, dyeing, and printing. These dyes can consume the dissolved oxygen required by aquatic life and some of them have direct toxicity to microbial populations and even can be toxic and/or carcinogenic to mammals. The problems associated with dye pollution could be reduced or minimized by physical, chemical, and biological processes, for example, by microbial degradation, chemical oxidation, coagulation, or filtration and membrane separation [1, 2]. But these processes have their disadvantages and limitations, such as high cost, generation of secondary pollutants, and poor removal efficiency. Thus adsorption has been found to be the most effective economic alternative with high potential for the removal and recovery of dyes from wastewater [1, 2].

* Corresponding author:
Sh. Sohrabnezhad
Department of Chemistry, Faculty of Science, University of Guilan, P.O. Box 1914, Rasht, Iran.
Tel +98 131 3233262
Fax +98 131 3233262
Email *sohrabnezhad@guilan.ac.ir*

Activated carbon is one of the most widely used adsorbents for this purpose [3, 4]. However, activated carbon suffers from high cost of production and regeneration [5]. Therefore, other adsorbents such as zeolites and mesoporous materials, pillared clays with higher surface areas are alternatives [6-8].

Synthetic and natural zeolites have become incurably important due to the wide range of their chemical and physical properties and have been used as adsorbents, molecular sieves, membranes, ion exchangers, and catalysts in the past decades. However, the application of zeolites for dye removal from wastewater has rarely been previously reported [9].

The discovery of ordered mesoporous materials has led to the explosive growth of research in the synthesis, characterization, and application of these materials [10-12]. As one of these materials, MCM-41 provides exciting opportunities for fundamental and applied studies on mesoporous materials. Such material is characterized by high surface area, high pore volume, as well as parallel and ideally shaped pore structures without the complications of a network. The cylindrical pore structure and high degree of pore symmetry found in ordered mesoporous silica are ideal for testing various existing adsorption and diffusion models [13-16]. Moreover, its unique pore structures also offer a special environment for chemical separations [17]. MCM-41 material may also have potential for liquid-phase separations and reactions. Among them, some applications involving liquid-phase systems have demonstrated the capability of MCM-41 in dealing with pollution problems, such as the removal of mercury and other heavy metals from water [18]. Ho et al. have shown that materials prepared by grafting amino- and carboxylic-containing functional groups onto MCM-41 might be a useful adsorbent for the removal of acid blue 25 and methylene blue dyes from waste water [19]. For these adsorption investigations, it was found that the interactions between adsorbents and surface functional groups of MCM-41 might play a key role on the determination of adsorption properties of the original and chemical modified MCM-41 samples.

In the last few years, various adsorbents have been applied for adsorption of various dyes from aqueous solutions. In these studies, mainly, single component systems have been investigated [20-25]. As most industrial wastewaters contain more than one pollutant, an investigation into the effects of multisolute systems on the adsorption capacity is practically important. Thus, in the present study, for a first time, we report single and binary component adsorption kinetic and thermodynamic for adsorption of MB and AU on AlMCM-41. Incorporation of aluminum into the structure of MCM-41 materials *via* isomorphous substitution of aluminum for silicon, generate ion exchange sites in this mesoporous molecular sieve [26, 27]. Therefore, cationic dyes such as methylene blue (MB) and auramine (AU) can be absorbed into AlMCM-41 by ion exchange method. The calcined AlMCM-41 has a specific surface area of 940 m^2/g and pore size of 24.4 Å [28]. These values are similar to the corresponding values for MCM-41 (surface area=1027 m^2/g and pore size=25.3 Å). Therefore, incorporation of aluminum does not alter considerably surface area and pore size of the AlMCM-41.

EXPERIMENTAL

Dyes

The dyes are MB and AU and were obtained from Merck. Chemical structures of the dyes are presented in Figure 1. For preparation of solutions, a stock solution with concentration of 10^{-3} M was prepared and the solutions for adsorption tests were prepared from the stock solution to the desired concentration (10^{-6}–10^{-5} M). The pH of solution was adjusted with HCl or NaOH (from Merck) solutions.

Preparation of AlMCM-41

The MCM-41 and AlMCM-41 materials were synthesized by a room temperature method with some modifications in the described procedure in literature [29]. We used tetraethylortho- silicate (TEOS from Merck) as a source of silicon and hexadecyltrimethylammonium bromide (HDTMABr from BOH) as a surfactant template for preparation of the mesoporous material. The molar composition of the reactants is as follows:

$$SiO_2 : 1.6EA : 0.215HDTMABr : 325H_2O$$

where EA stand for ethylamine. The prepared MCM-41 was calcined at 550 °C for 5 h to decompose the surfactant and obtain the white powder. This powder was used as the parent material to prepare AlMCM-41 by ion-exchange method with 0.1 M solution of Al_2 $(SO4)_3 \cdot 18H_2O$ (from Merck).

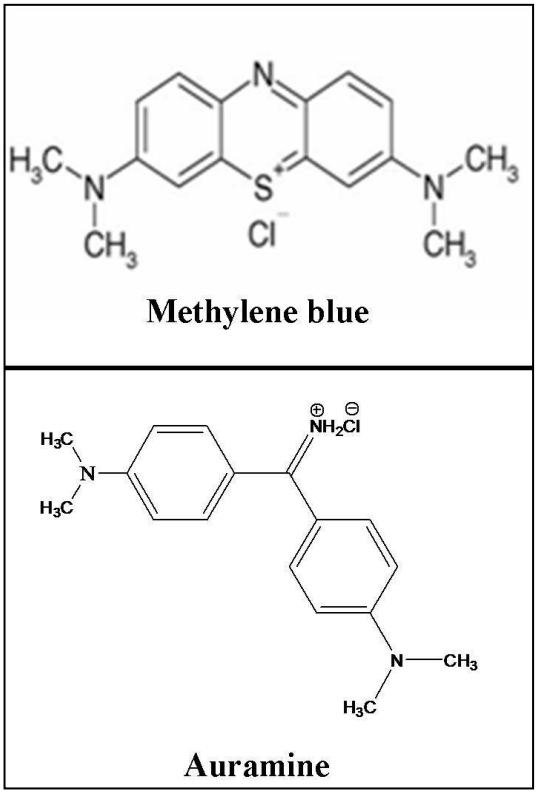

Fig. 1. Chemical structures for methylene blue (MB) and auramine (AU).

Adsorption test

Adsorption kinetics and isotherm experiments for the samples were undertaken in a batch reactor with 250 ml capacity provided with water circulation arrangement to maintain the temperature at desired value. Adsorption of the dyes was performed by shaking 0.005 g of AlMCM-41 in 200 ml of the solutions with varying concentrations (10^{-6}–10^{-5} M) at 25 and 40 ˚C. The samples were collected by separation of AlMCM-41 from solution using a centrifuge. Concentration of dyes was determined spectrophotometrically by measuring absorbance at 664 and 432 nm for λ_{max} of MB and AU, respectively. The data obtained from the adsorption tests were used to calculate the adsorption capacity, q_t (mol/g), of the adsorbent by a mass–balance relationship, which represents the amount of adsorbed dye per amount of the dry adsorbent:

$$q_t = \frac{(C_o - C_t)V}{W} \qquad (1)$$

where C_0 and C_t are concentrations of the dyes in solution (mol/dm^3) at time t = 0 and t = t, respectively. V is the volume of the solution (dm^3), and W is weight of the dry adsorbent (g).

RESULTS AND DISCUSSION

Adsorption in single component systems

Figure 2 demonstrates the dynamic adsorption of MB and AU onto AlMCM-41 at 25 and 40 ° C. As can be seen, the adsorption of MB and AU on the adsorbent reaches equilibrium approximately at 300 minutes. This time is very shorter than corresponding time for natural zeolites [23, 30]. Also, one can see that the adsorption of MB and AU is fast at initial times and then approaches equilibrium at longer times. The time profile for adsorption of the dyes is single, smooth and continuous curve leading to saturation, suggesting the possible monolayer coverage of the dyes on surface of the adsorbent. Also, AlMCM-41 exhibits higher adsorption for MB than AU due to its smaller molecular size than AU, which can be seen in Figure 1. For the same adsorbent, large size molecules will not easily penetrated into the inner pores of the adsorbent, resulting in lower adsorption capacity [23]. Similar results have been reported for adsorption of MB and AU on various adsorbents [23, 28]. The adsorption capacity at equilibrium for adsorption of MB and AU in initial concentration of 8×10^{-6} M at 25 ºC is 2.07×10^{-4} and 1.15×10^{-4} mol/g, respectively. Then, it can be concluded that the adsorption capacity of AlMCM-41 for MB and AU is very higher than natural zeolite.

As seen from Figure 2 that temperature will influence the adsorption capacity. For the dyes, the adsorption at 25 ˚C is higher than that at 40 ˚C, suggesting the exothermic characteristic of the adsorption.

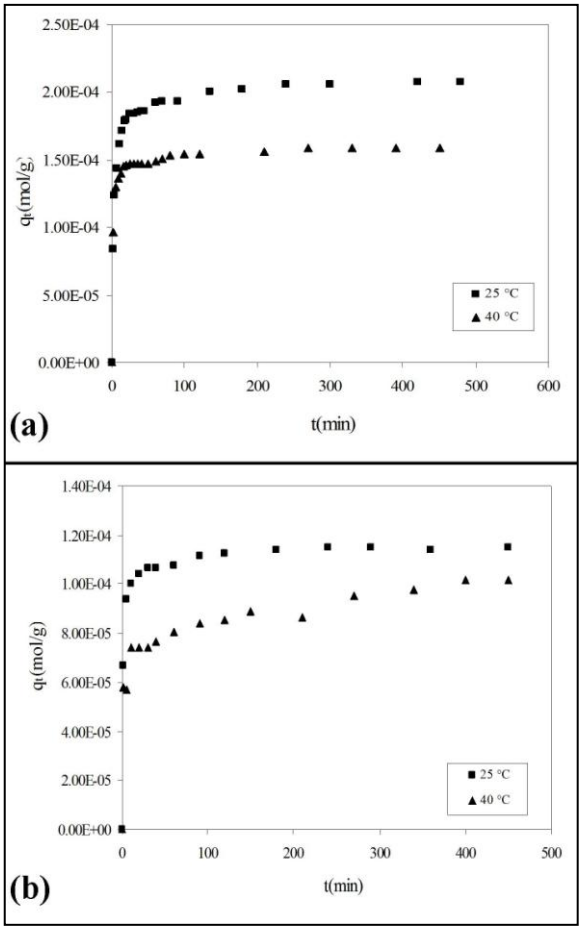

Fig. 2. Dynamic adsorption of MB and AU onto AlMCM-41 at 25 and 40 ºC for (A) MB and (B) AU in initial concentration of 8.0×10^{-6}.

Adsorption isotherm in single component systems

An adsorption isotherm shows how the adsorbate molecules partition between the liquid and solid phases when the adsorption process reaches equilibrium conditions. The adsorption isotherm is fundamental in describing the interactive behavior between solutes and adsorbent, and is important in the design of adsorption systems [23]. Several adsorption isotherms are available and two important isotherms used in this study. The Langmuir adsorption is based on the assumption of monolayer adsorption on a structurally homogeneous adsorbent, where all the sorption sites are identical and energetically equivalent. Where in, the adsorption occurs at specific homogeneous sites within the adsorbent and once a dye molecule occupies a site, no further adsorption can take place at that site. The equation is as follows:

$$q_e = \frac{K_L q_{max} C_e}{1 + K_L C_e} \qquad (2)$$

where q_e is the equilibrium dye concentration on adsorbent (mol/g), C_e is the equilibrium concentration of the dye in solution (mol/l), q_{max} is the monolayer adsorption capacity of adsorbent (mol/g). The Langmuir constant (K_L) is a measure of the affinity between adsorbate and adsorbent and related to the free energy of adsorption [21]. A linear expression for the Langmuir equation is:

$$\frac{C_e}{q_e} = \frac{1}{q_{max} K_L} + \frac{C_e}{q_{max}} \qquad (3)$$

A plot of C_e/q_e *versus* C_e gives a straight line of slope $1/q_{max}$ and intercepts $1/q_{max}K_L$.

The Freundlich adsorption isotherm is one of the most widely used empirical equation, which fits with the experimental data over a wide range of concentrations. This is based on the assumption that the adsorption surface is heterogeneous and exponential distribution of active sites. It also assumes that an unlimited number of unreacted sites are available [30-31]. This isotherm is as follows:

$$q_e = K_F C_e^{1/n} \qquad (4)$$

Where K_F and n are Freundlich adsorption constants, indicative of the adsorption extent and the degree of nonlinearity between solution concentration and adsorption, respectively. The Freundlich equation in logarithmic form can be given as:

$$\log q_e = \log K_F + \frac{1}{n} \log C_e \qquad (5)$$

Plot of log q_e *versus* log C_e gives K_F and n constants. Figures 3 and 4 show, the linearized Langmuir model for adsorption of MB and AU onto AlMCM-41 at 25 and 40 ºC. The parameters obtained from the experimental data using the two isotherms and the related correlation coefficients

are presented in Table 1. One can see that regression coefficients obtained from the Langmuir isotherm are closer to unity than the Freundlich isotherm. Then, it can be concluded that the adsorption of both dyes obeys from Langmuir isotherm. Based on the Langmuir isotherm, the maximum adsorption of MB and AU are $2.08\times10^{-4}$and 1.39×10^{-4} mol/g, respectively at 25˚C.

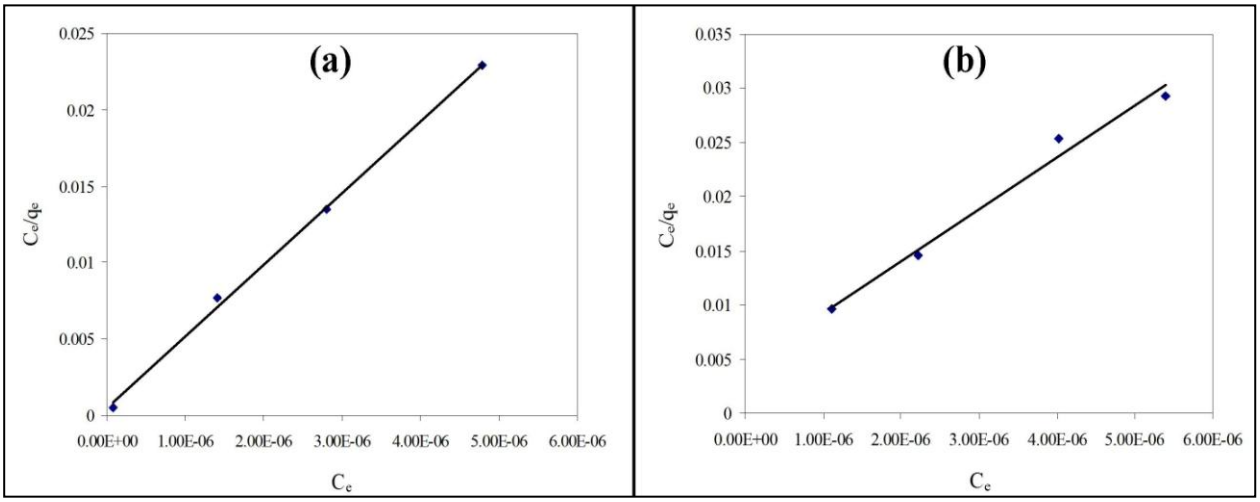

Fig. 3. Langmuir plots for adsorption of MB onto AlMCM-41at (A) 25 ˚C; (B) 40 ˚C.

Table 1. Parameters for adsorption of MB and AU on AlMCM-41 in single component systems.

Dyes	Temperature (˚C)	Langmuir isotherm			Freundlich isotherm		
		q_{max} (mol/g)	K_L (1/mol)	R^2	K_F (mol/g)	1/n	R^2
AU	25	1.39×10^{-4}	1.14×10^{6}	0.9842	8.25×10^{-4}	0.160	0.8505
	40	5.92×10^{-4}	3.79×10^{4}	0.9981	3.29	0.857	0.9998
MB	25	2.08×10^{-4}	9.58×10^{6}	0.9982	5.08×10^{-4}	0.072	0.9470
	40	2.08×10^{-4}	1.06×10^{6}	0.9854	4.67×10^{-3}	0.268	0.9363

Based on the adsorption constant in the Langmuir isotherm (K_L), thermodynamic parameters (ΔG°, ΔH° and ΔS°) for adsorption of MB and AU onto AlMCM-41 were calculated using Eqs. (6–8) and are given in Table 2.

$$\Delta G^\circ = -RT \ln K_L \quad (6)$$

$$\Delta H^\circ = -R\left(\frac{T_2 T_1}{T_2 - T_1}\right)\ln\frac{K_{L1}}{K_{L2}} \quad (7)$$

$$\Delta S^\circ = \frac{\Delta H^\circ - \Delta G^\circ}{T} \quad (8)$$

As can be seen, the adsorption process is spontaneous with the negative value of ΔG°. The standard enthalpy change (ΔH°) for the adsorption of the dyes on AlMCM-41 is negative indicating that the process is exothermic in nature with ΔH° of -175.97 and -113.80 kJ/mol for RB and AU, respectively.

Adsorption kinetics in single component systems

The kinetic study of the adsorption processes provides useful data regarding the efficiency of adsorption and feasibility of scale-up operations. To evaluate the effectiveness of an adsorbate, studies on kinetics of adsorption are also needed [30].

The kinetics of adsorption can be described using several models. A simple kinetic model is the pseudo-first-order equation [28]:

$$\frac{dq_t}{dt} = k_1(q_e - q_t) \quad (9)$$

where k_1 is rate constant for pseudo-first-order adsorption. After definite integration by applying the initial conditions $q_t = 0$ at $t = 0$ and $q_t = q_t$ at $t = t$, equation 9 becomes:

$$\ln(q_e - q_t) = \ln(q_e) - k_1 t \quad (10)$$

The above linear equation can usually be used to estimate q_e from intercept and k_1 from the slope. A pseudo-second-order equation can be expressed as follows:

$$\frac{dq_t}{dt} = k_2(q_e - q_t)^2 \quad (11)$$

where k_2 is rate constant for pseudo-second-order adsorption. After definite integration by applying the initial conditions, we have a linear form as:

$$\frac{t}{q_t} = \frac{1}{k_2 q_e^2} + \frac{1}{q_e}t \quad (12)$$

Table 2. Thermodynamic parameters for adsorption of MB and AU on AlMCM-41 in single component system.

Dyes	Temperature (°C)	ΔG° (kJ/mol)	ΔH° (kJ/mol)	ΔS° (J/mol K)
AU	25	-34.55	-175.97	-474.57
	40	-27.43		
MB	25	-39.82	-113.80	-248.28
	40	-36.10		

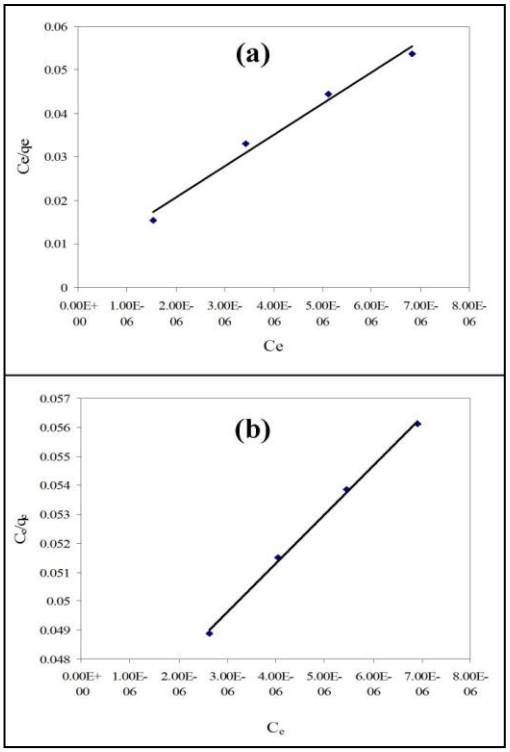

Fig. 4. Langmuir plots for adsorption of AU onto AlMCM-41at (A) 25 °C; (B) 40 °C.

The plot of *t*/*qt versus* time gives straight lines. The values for q_e and k_2 can be calculated from the slope and intercept. Figure 5 represents plot of pseudo-second-order kinetic model for adsorption of MB and AU at 25 and 40 ˚C. Also, the kinetic parameters obtained from the models are given in Table 3. The correlation coefficients are closer to unity for pseudo-second-order kinetics than that for the pseudo-first-order kinetics. This suggests that the adsorption of MB and AU onto AlMCM-41can be represented better by the pseudo-second-order model.

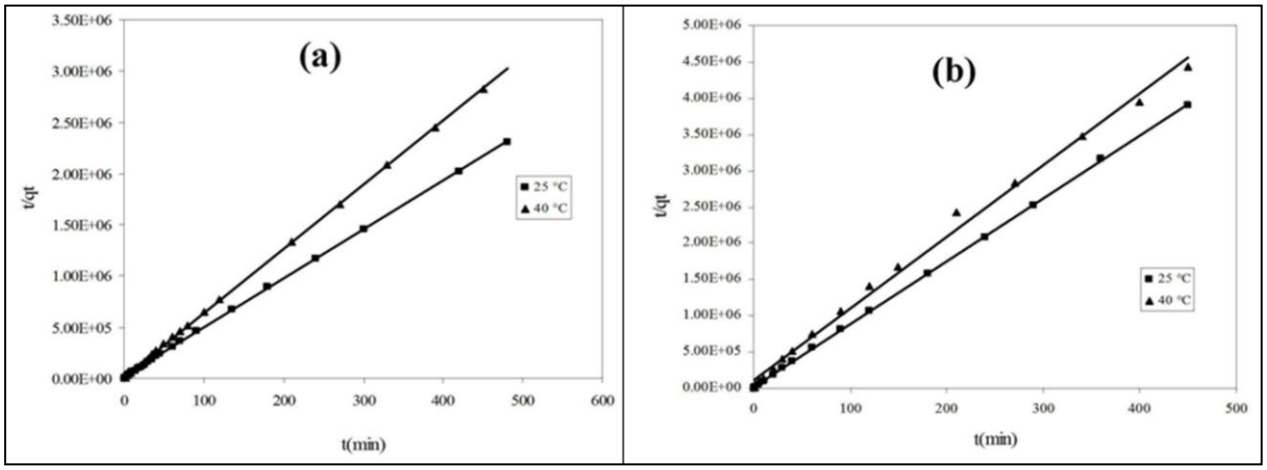

Fig. 5. Pseudo-second-order kinetics for adsorption of MB and AU onto AlMCM-41 at 25 and 40 °C (A) MB; (B) AU.

Table 3. Kinetic parameters for adsorption of MB and AU on AlMCM-41 in single component system.

Dyes	Temperature (˚C)	Experimental q_e (mol/g)	First-order kinetics			Second-order-kinetics		
			q_{max} (mol/g)	K_L (1/mol)	R^2	K_F (mol/g)	1/n	R^2
AU	25	1.15×10^{-4}	1.88×10^{-5}	0.010	0.6314	1.15×10^{-4}	0.9999	2.04×10^{5}
	40	1.01×10^{-4}	3.98×10^{-5}	0.006	0.8337	1.01×10^{-4}	0.9955	5.35×10^{4}
MB	25	2.07×10^{-4}	0.9999	6.86×10^{4}	2.09×10^{-4}	0.8604	0.011	4.45×10^{-5}
	40	1.58×10^{-4}	0.9999	1.34×10^{5}	1.59×10^{-4}	0.9415	0.010	1.82×10^{-5}

The intraparticle diffusion model was also applied to the kinetic adsorption. The rate parameter for the intraparticle diffusion is calculated using the following equation:

$$q_t = k_P \left(t^{1/2} \right) \qquad (13)$$

where k_p is the intraparticle diffusion rate constant. It is generally found that the plot of q_t against $t^{1/2}$ may present a multilinearity, which indicates that two or more steps occur in the adsorption processes [17].

Figure 6 shows the diffusion modeling on kinetics of the dyes adsorption on AlMCM-41. One can see that the adsorption of MB and AU occurs is in two stages. The first one is attributed to external surface adsorption and the second one should be intraparticle diffusion process. Previous studies have demonstrated that a two-step is involved in the adsorption process of dyes on several adsorbents [22, 32].

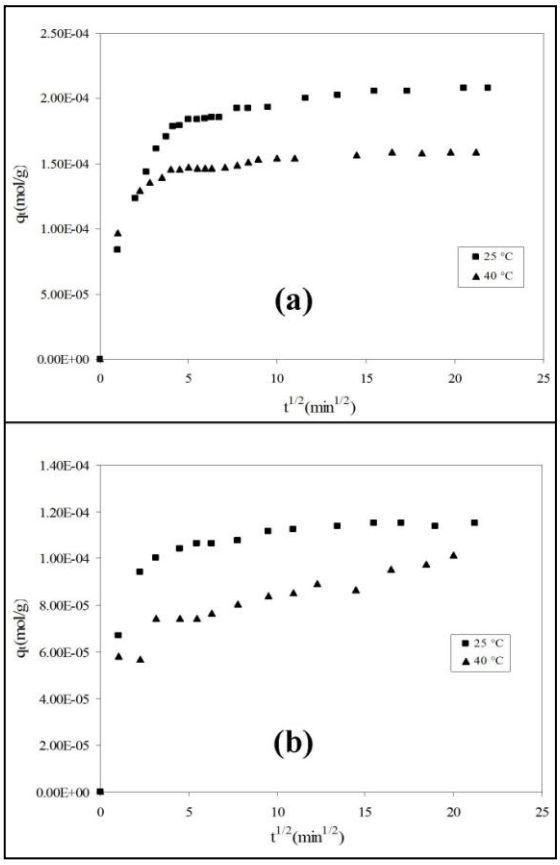

Fig. 6. Intraparticle diffusion modeling for adsorption of MB and AU onto AlMCM-41at 25 and 40 ºC (A) MB; (B) AU.

Effect of solution pH on single component systems

It is known that adsorption of dyes onto adsorbents is influenced by pH of solution [28]. Figure 7 demonstrates the dynamic adsorption of MB and AU onto AlMCM-41 at different initial pH and 25 °C. As can be seen, amount of MB adsorption initially increases as the pH is increasing and then decreases. When pH of solution is changed from 4 to 6.5, the adsorption increases from 6.71×10^{-5} to 2.08×10^{-4} mol/g. The presence of excess H^+ ions competing with the cationic dyes for adsorption sites in acidic solutions. For this reason the amount of MB and AU adsorption decrease in acidic solutions. It is clear that the amount of AU adsorption greatly increasing as the pH is increasing. When pH of solution is changed from 6.5 to 10, the adsorption will increases from 1.11×10^{-4} to 2.08×10^{-4} mol/g.

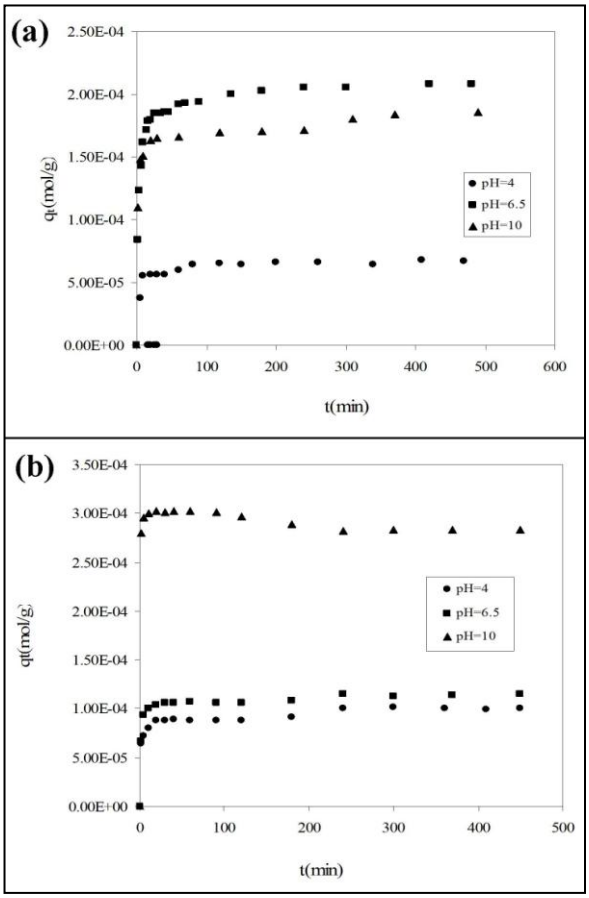

Fig. 7. Dynamic adsorption of MB and AU onto AlMCM-41 in various pH at 25 ºC for (A) MB; (B) AU.

Adsorption in binary component system

- **Adsorption isotherm in binary component system**

Figure 8 demonstrates a comparison of MB and AU adsorption onto AlMCM-41 in single and binary component systems at 25 and 40 ˚C for initial concentration of 4×10^{-6} M. It is clear that the adsorption is reduced in binary component system, which suggests a competitive adsorption. During the process, adsorption reaches an equilibrium adsorption of 1.41×10^{-4} and 3.92×10^{-5} mol/g at initial concentration of 4×10^{-6} M for MB and AU at 25 ˚C.

Figure 9 represents the linearized Langmuir isotherm for adsorption of MB onto the adsorbent at 25 and 40 °C in binary component system. It is clear that similar to single component systems, the competitive adsorption data is mainly fitting in the Langmuir model. Table 4 compares the results obtained by fitting the Langmuir and Frundlich isotherms for competitive adsorption of MB and AU. By comparing the results in Tables 1 and 4, one can see that the Langmuir constant (K_L) for adsorption of MB and AU in binary component system is lower than single component systems. Also, using equations 6-8, thermodynamic parameters (ΔG°, ΔH° and ΔS°) for adsorption of MB and AU in binary component system were calculated (Table 5). As can be seen, similar to single component systems, the adsorption is exothermic.

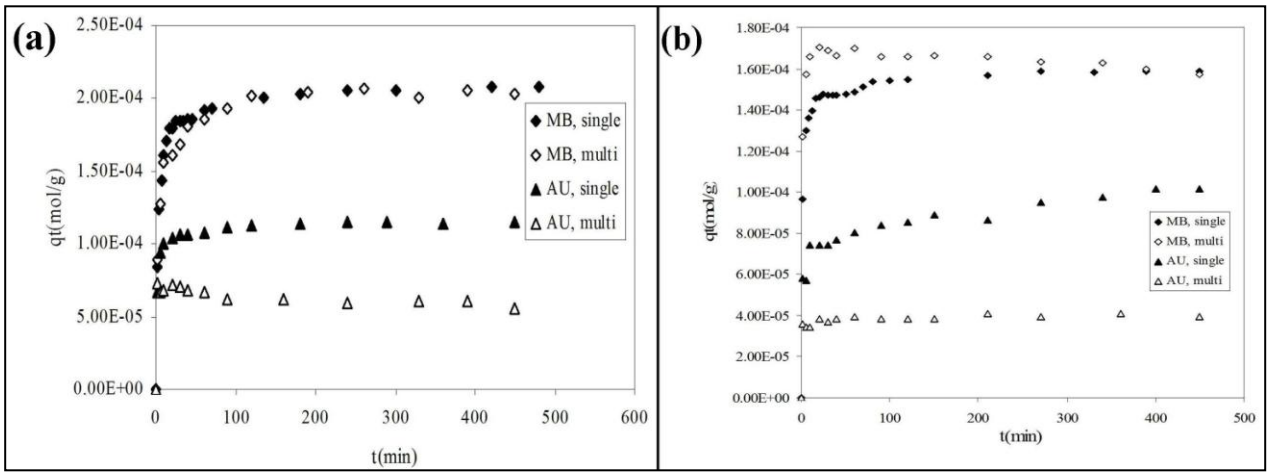

Fig. 8. Comparison of MB and AU adsorption in single and binary component systems at (A) 25 ºC; (B) 40 ºC.

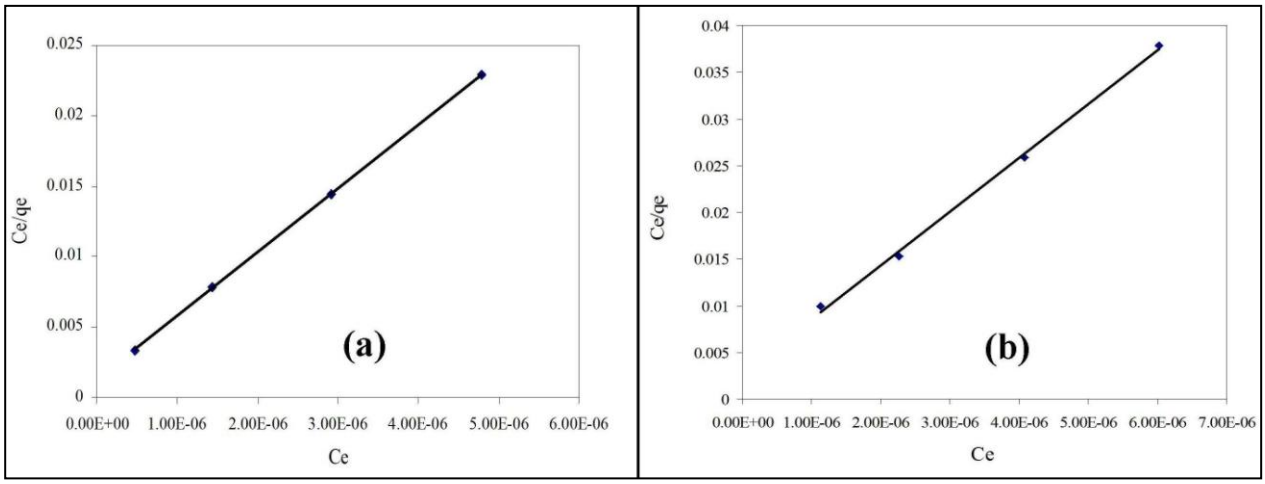

Fig. 9. Langmuir plots for adsorption of MB onto AlMCM-41 in binary component system at different temperatures (A) 25 ˚C; (B) 40 ˚C.

Table 4. Parameters for adsorption of MB and AU on AlMCM-41 in binary component system.

Dyes	Temperature (˚C)	Langmuir isotherm			Freundlich isotherm		
		q_{max} (mol/g)	K_L (1/mol)	R^2	K_F (mol/g)	1/n	R^2
AU	25	0.8907	0.351	3.56×10^{-3}	0.9842	4.29×10^{5}	7.32×10^{-5}
	40	0.9824	0.571	3.54×10^{-2}	0.9857	1.40×10^{5}	8.12×10^{-5}
MB	25	0.9555	0.174	1.83×10^{-3}	0.9999	3.47×10^{6}	2.21×10^{-4}
	40	0.8437	0.195	1.75×10^{-3}	0.9978	2.05×10^{6}	1.73×10^{-4}

Table 5. Thermodynamic parameters for adsorption of MB and AU on AlMCM-41 in binary component system.

Dyes	Temperature (˚C)	ΔG° (kJ/mol)	ΔH° (kJ/mol)	ΔS° (J/mol K)
AU	25	-32.13	-57.89	-86.45
	40	-30.83		
MB	25	-37.31	-27.20	33.92
	40	-37.81		

- **Adsorption kinetics in binary component system**

Plot of pseudo-second-order kinetic model for adsorption of MB and AU at 25 and 40 °C in binary component system have been demonstrated in Figure 10. Also, in Table 6, results for the competitive adsorption are compared. It is clear that pseudo-second-order kinetic model show much better correlation coefficients, close to ideal value in all cases. Thus, similar to single component systems, the adsorption of the basic dyes on the adsorbent in binary component system follows the pseudo-second-order kinetics. Also, it is clear that the second-order rate constant for adsorption of AU is higher than that of MB.

The intraparticle diffusion model (equation 13) was also applied to the adsorption kinetics of MB and AU in binary component system. Figure 11 shows the diffusion modeling on kinetics of the adsorption. It is clear that, similar to single component systems, the adsorption of MB and AU occurs in two stages.

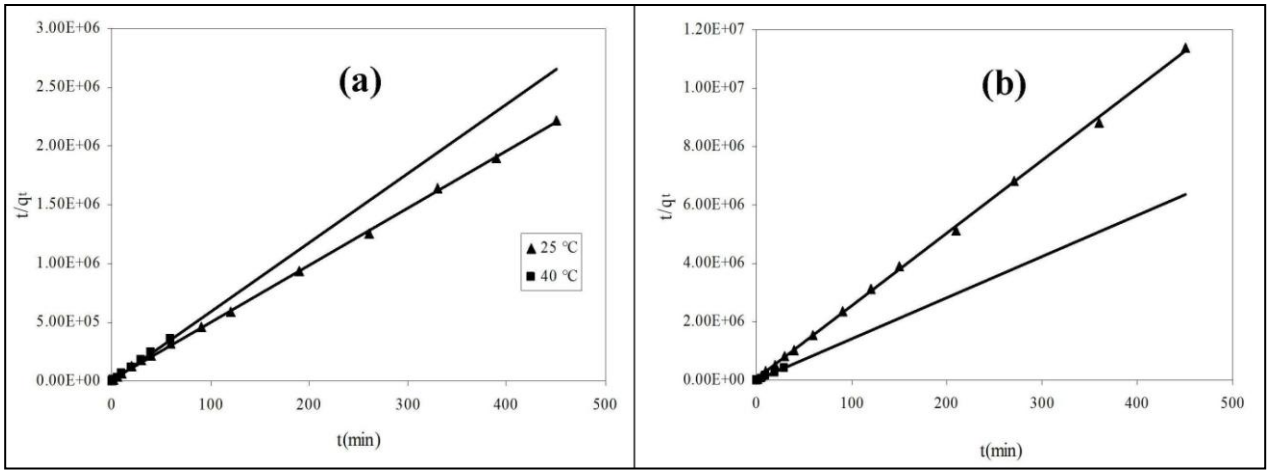

Fig. 10. Pseudo-second-order kinetics for adsorption of MB and AU onto AlMCM-41 in binary component system at 25 and 40 °C (A) MB; (B) AU.

Table 6. Kinetic parameters for adsorption of MB and AU on AlMCM-41 in binary component system

Dyes	Temperature (˚C)	Experimental q_e (mol/g)	First-order kinetics			Second-order-kinetics		
			q_{max} (mol/g)	K_L (1/mol)	R^2	K_F (mol/g)	1/n	R^2
AU	25	3.92×10^{-5}	7.51×10^{-6}	0.0066	0.5652	3.90×10^{-5}	3.95×10^{5}	0.9990
	40	2.62×10^{7}	2.74×10^{-5}	0.5989	2.1286	5.78×10^{-2}	2.56×10^{-5}	0.9989
MB	25	1.41×10^{-4}	4.07×10^{-5}	0.0071	0.7427	1.39×10^{-4}	8.40×10^{4}	0.9993
	40	1.16×10^{-4}	0.4745	0.0038	5.04×10^{-5}	1.14×10^{-4}	1.53×10^{5}	0.9996

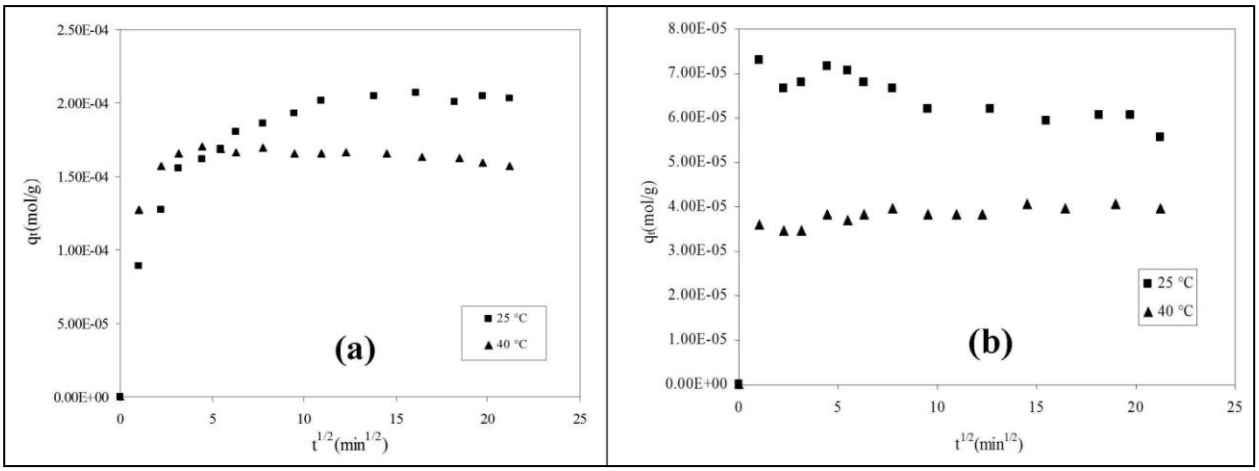

Fig. 11. Intraparticle diffusion modeling for adsorption of MB and AU onto AlMCM-41 in binary component system at 25 and 40 ºC (A) MB; (B) AU.

- **Effect of solution pH on binary component system**

Figure 12 shows the dynamic adsorption of MB and AU with initial concentration of 8×10^{-6} M onto AlMCM-41 at three different pH and 25 °C in binary component system. It is clear that, similar to single component system, the amount of MB and AU adsorption greatly increasing as the pH is increasing. When pH of solution is changed from 6.5 to10, the adsorption will change from 2.03×10^{-4} to 3.06×10^{-4} mol/g and from 5.56×10^{-5} to 1.08×10^{-4} mol/g for MB and AU, respectively.

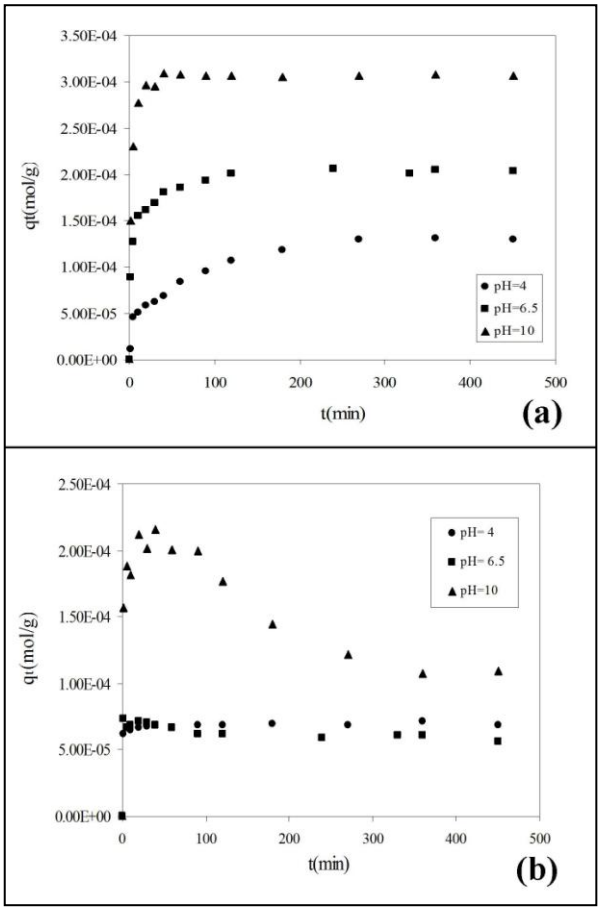

Fig. 12. Dynamic adsorption of MB and AU onto AlMCM-41in binary component system in various pH at 25 ºC (A) MB; (B) AU.

CONCLUSIONS

The AlMCM-41 was applied for single and binary component adsorption systems of two basic dyes, MB and AU. It was found that the adsorbent exhibits higher adsorption capacity for MB than AU due to the difference in molecular size. The maximal adsorption capacities for MB and AU are 2.07×10^{-4} and 1.15×10^{-4} mol/g at 25°C, respectively. For single and binary component systems, the adsorption data could be fairly fitted by the Langmuir model. Kinetics of the adsorption is better described by the pseudo-second-order model with two-step diffusion process.

REFERENCES

[1] Gupta, V.K., Mittal, A., Krishnan, L., Mittal, J. (2006). Adsorption treatment and recovery of the hazardous dye, Brilliant Blue FCF, over bottom ash and de-oiled soya. *J. Colloid Interface Sci*, 293, 16-26.

[2] Han, R., Wang, Y., Zou, W., Wang, Y., Shi, J. (2007). Comparison of linear and nonlinear analysis in estimating the Thomas model parameters for methylene blue adsorption onto natural zeolite in fixed-bed column, *J. Hazard. Mater*, 145, 331-335.

[3] Gupta, V.K., Mittal, A., Jain, R., Mathur, M., Sikarwar, S. (2006). Adsorption of Safranin-T from wastewater using waste materials— activated carbon and activated rice husks, *J. Colloid Interface Sci*, 303, 80-86.

[4] Wang, S., Zhu, Z.H., Coomes, A., Haghseresht, F., Lu, G.Q. (2005). The physical and surface chemical characteristics of activated carbons and the adsorption of methylene blue from wastewater. *J. Colloid Interface Sci*, 284, 440-446.

[5] El-Sharkawy, E.A., Soliman, A.Y., Al-Amer, K.M. (2007). Comparative study for the removal of methylene blue via adsorption and photocatalytic degradation. *J. Colloid Interface Sci*, 310, 498-508.

[6] Petkowicz, D.I., Brambilla, R., Radtke, C., Silva da, C.D., Rocha da, Z.N., Pergher, S.B.C., Santos dos, J.Z.H. (2009).

photodegradation of methylene blue by in situ generatwd titania supported on a NaA zeolite, *Applied Catalysis A: General* 357, 125-134.

[7] Jin, X., Jiang, M-Q., Shan, H-Q., Pei, Zh-G., Chen, Z. (2008). adsorption of methylene blue and orange II onto unmodified and surfactant-modified zeolite. *J. Colloid Interface Sci*, 328, 243-247.

[8] Wang, Sh., Li, H., Xu, L. (2006). Application of zeolite MCM-22 for basic dye removal from wastewater. *J. Colloid Interface Sci*, 295, 71-78.

[9] Sohrabnezhad, Sh., Pourahmad, A., Radaee, E. (2009). Photocatalytic degradation of basic blue 9 by CoS nanoparticles supported on AlMCM-41 material as a catalyst. *J. Hazmat. Mater*, 170, 184-190.

[10] Zhao, X.S., Lu, G.Q., Millar, G.J. (1996). Advances in mesoporous sieve MCM-41. *Ind. Eng. Chem. Re*s, 35, 2075-2090.

[11] Corma, A. (1997).From microporous to mesoporous molecular sieve materials and their use in catalysis, *Chem, Rev*, 97, 2373-2419.

[12] Ying, J.Y., Mehnert, C.P., Wong, M.S. (1999). Synthesis and applications of supramolecular-templated mesoporous materials, *Angew. Chem. Int. Ed*, 38, 56-77.

[13] Selvam, P., Bhatia, S.K., Sonwane, C.G. (2001). Recent advances in processing and characterization of periodic mesoporous MCM-41 silicate molecular sieves, *Ind. Eng. Chem. Res*, 40, 3237-3261.

[14] Storck, S., Bretinger, H., Maier, W.F. (1998). Characterization of micro and mesoporous solids by physisorption methods and pore-size analysis, *Appl. Catal. A: General*, 174, 137-146.

[15] Choma, J., Jaroniec, M., Kloske, W. (2001). Critical appraisal of classical methods for determination of mesopore size distributions of MCM-41 materials, *Appl. Surf. Sci*, 196, 216-223.

[16] Ribeiro Carrott, M.M.L., Candeias, A.J.E., Ravikovitch, P.I., Neimark, A.V., Sequeira, A.D. (2001). Adsorption of nitrogen, neopentane, n-hexane, benzene, and methanol for the evaluation of pore sizes in silica grades of MCM-41, *Micropore. Mesopor. Mater*, 47, 323-337.

[17] Wloch, J., Rozwadowski, M., Lezanska, M., Erdmann, K. (2002). Analysis of the pore structure of the MCM-41 materials, *Appl. Surf. Sci*, 191, 368-374.

[18] Liu, J., Feng, X., Fryxell, G.E., Wang, L.Q., Kim, A.Y., Gong, M. (1998). Hybrid mesoporous materials with functionalized monolayers, *Adv. Mater*, 10, 61-65.

[19] Ho, K.Y., McKay, G., Yeung, K.L. (2003). Selective adsorbents from ordered mesoporous silica, *Langmuir*, 19, 3019-3024.

[20] Meshko, V., Markovska, L., Mincheva, M., Rodrigues, A.E. (2001). Adsorption of basic dyes on granular activated carbon and natural zeolite, *Water Res*, 35, 3357–3366.

[21] Wang, S., Li, H., Xu, L. (2006). Application of zeolite MCM-22 for basic dye removal from wastewater, *J. Colloid and Interface Sci*, 295, 71-78.

[22] Vadivelan, V., Kumar, K.V. (2005). Equilibrium, kinetics, mechanism, and process design for the sorption of methylene blue onto rice husk, *J. Colloid and Interface Sci*, 286, 90-100.

[23] Wang, S., Zhu, Z.H. (2006). Characterisation and environmental application of an Australian natural zeolite for basic dye removal from aqueous solution, *J. Hazard. Mater*, 136, 946–952.

[24] Yener, J., Kopac, T., Dogu, G., Dogu, T. (2006). Adsorption of Basic Yellow 28 from aqueous solutions with clinoptilolite and amberlite, *J. Colloid and Interface Sci*, 294, 255-264.

[25] Alpat, S.K., Ozbayrak, O., Alpat, S., Akcay, H. (2008). The adsorption kinetics and removal of cationic dye, Toluidine Blue O, from aqueous solution with Turkish zeolite, *J. Hazard. Mate*, 151, 213–220.

[26] Wei, D., Wang, H., Feng, X., Chuch, W., Ravikovitch, P., Lyubovsky, M., Li, C., Tekeguchi, T., Holler, G.L. (1999). Synthesis and characterization of vanadium-substituted mesoporous molecular sieves, *J. Phys. Chem. B,* 103, 2113-2121.

[27] Zanjanchi, M.A., Asgari, Sh. (2004). Incorporation of aluminum into the framework of mesoporous MCM-41: the contribution of diffuse reflectance spectroscopy, *Solid State Ionics,* 171, 277-282.

[28] Zanjanchi, M.A., Ebrahimian, A., Alimohammadi, Z. A spectroscopic study on the adsorption of cationic dyes into mesoporous AlMCM-41 materials, *Optical Materials*, 29, 794–800

[29] Cai, Q., Luo, Zh-Sh., Pang, W.Q., Fan, Yu-W., Chen, Xi-H., Cui, Fu-Zh. (2001). Dilute solution routes to various controllable morphologies of MCM-41 silica with a basic medium, *Chem. Mater*, 13, 258–263.

[30] Wang, S., Li, H., Xie, S., Liu, S., Xu, L. (2006). Physical and chemical regeneration of zeolitic adsorbents for dye removal in wastewater treatment, *Chemosphere*, 65, 82–87.

[31] Kumar, K.V., Ramamurthi, V., Sivanesan, S. (2005). Modeling the mechanism involved during the sorption of methylene blue onto fly ash, *J. Colloid and Interface Sci*, 284, 14-21.

[32] Selvam, P.P., Preethi, S., Basakaralingam, P., Thinakaran, N., Sivasamy, A., Sivanesan, S. (2008).Removal of rhodamine B from aqueous solution by adsorption onto sodium montmorillonite, *J. Hazard. Mater*, 155, 39-44.

Cite this article as: Sh. Sohrabnezhad *et al.*: Nanodimensional AlMCM-41 material for adsorption of dyes: Thermodynamic and kinetic studies.
Int. J.Nano Dimens. 4(2): 91-104, Autumn 2013